INSTITUTE OF PHYSICS PUBLISHING JOURNAL OF PHYSICS: CONDENSED MATTER

J. Phys.: Condens. Matter **15** (2003) S3569–S3580 PII: S0953-8984(03)66673-7

Defying gravity with entropy and electrostatics: sedimentation of charged colloids

René van Roij

Institute for Theoretical Physics, Utrecht University, Leuvenlaan 4, 3584 CE Utrecht, The Netherlands

Received 23 July 2003, in final form 22 September 2003
Published 20 November 2003
Online at stacks.iop.org/JPhysCM/15/S3569

Abstract

We combine hydrostatic equilibrium with Donnan equilibrium to identify three different regimes of sedimentation equilibrium in suspensions of highly charged colloids. In the low-density regime the familiar exponential (barometric) distribution is recovered, in an intermediate density regime the profile is found to be linear with height, and in the high-density regime it is exponential again but with a gravitational length that is increased by a factor $Z + 1$, where Z is the colloidal charge number. The nonbarometric distributions are explained in terms of macroscopic electric fields, generated by macroscopic charge separation as calculated by Poisson–Boltzmann theory.

1. Introduction

Fluids in the Earth's gravity field face a competition between minimal energy (all particles at the bottom) and maximal entropy (a homogeneous distribution of particles). The balance between these two competing tendencies is governed by hydrostatic equilibrium, which on a macroscopic scale and for a one-component fluid can be cast in the form [1]

$$\frac{\mathrm{d}P(\rho(x))}{\mathrm{d}x} = -mg\rho(x), \tag{1}$$

where $P(\rho)$ is the pressure of the bulk fluid at number density ρ, x is the height above the surface, m is the mass of the particles, and g the gravitational acceleration. For a given bulk equation of state, $P(\rho)$, equation (1) is a first-order differential equation for the equilibrium density profile $\rho(x)$, and the constant of integration is determined by the total number of particles in the system. Conversely, equation (1) can be used to obtain the equation of state by integrating a known equilibrium density profile $\rho(x)$ [2]. In this paper we take the former approach. For a sufficiently dilute fluid, for which the ideal-gas equation of state $P = kT\rho$ holds (with kT the thermal energy, assumed uniform in space here), equation (1) is easily solved and yields the familiar barometric height distribution

$$\rho(x) = \rho_0 \exp(-x/L), \qquad L = \frac{kT}{mg}, \tag{2}$$

0953-8984/03/483569+12$30.00

where ρ_0 is a normalising constant determined by the total amount of gas in the system. The so-called gravitational length L sets the length scale of the spatial inhomogeneity of the gas, and is of the order of kilometres for atomic gases at atmospheric temperatures.

In this contribution we use equation (1) to describe sedimentation equilibrium in colloidal suspensions, even though such systems are *not* one-component fluids—they consist at least of a molecular solvent and a colloidal species. This is possible provided one regards $P(\rho)$ as the osmotic equation of state, and m as the buoyant mass of the colloidal particles [3–5]. The focus of this paper is on suspensions of charged colloids, where the constraint of global charge neutrality is responsible for a rather richly structured osmotic pressure $P(\rho)$, even on the (almost) ideal-gas level as first described by Donnan. The tendency to maintain local charge neutrality, and the possibility to violate it, turn out to seriously affect the competition between potential energy and entropy, which usually determine sedimentation equilibrium.

This paper is organised as follows. In section 2 we will first present a rederivation of the Donnan expression for $P(\rho)$, which we combine with the hydrostatic equilibrium condition (1) in section 3. It will then turn out to be necessary to include the Maxwell stress to the force balance of equation (1), which we discuss in section 4. In section 5 we end with a discussion on the experimental realizability of the phenomenon discussed, and with some conclusions.

2. The homogeneous bulk system

Consider a bulk system of negatively charged colloidal spheres, each carrying a homogeneous surface charge $-Ze$ where e is the proton charge. The number density of colloids is ρ. The colloids are suspended in a structureless incompressible molecular medium, together with monovalent cations and anions at concentrations c_+ and c_-, respectively. Global charge neutrality dictates that

$$Z\rho = c_+ - c_-. \tag{3}$$

We imagine this suspension in osmotic (Donnan) equilibrium with a (neutral) reservoir of the cations and anions at a total concentration $2c_s$. Within the ideal-gas approximation the chemical potential of the cations and anions is therefore given by

$$\mu_\pm = kT \log(c_s \Lambda_\pm^3), \tag{4}$$

where $\Lambda_\pm$ denotes the (irrelevant) thermal wavelength of the ions. Here the average (macroscopic) electrostatic potential is gauged to be vanishing in the reservoir. This average potential, however, is nonzero (and negative) in the suspension because of the presence of the negative colloids. Denoting this so-called Donnan potential by ψ, we find for the chemical potential of the ions in the suspension (again assuming ideal-gas behaviour)

$$\mu_\pm = kT \log(c_\pm \Lambda_\pm^3) \pm e\psi. \tag{5}$$

Because of the Donnan equilibrium the chemical potentials of the ions in the reservoir and the suspension are equal, and it follows directly from equations (4) and (5) that

$$c_\pm = c_s \exp(\mp\phi), \tag{6}$$

where we have introduced the dimensionless Donnan potential

$$\phi = \frac{e\psi}{kT}. \tag{7}$$

The charge neutrality condition, equation (3), imposes ϕ to satisfy

$$-\sinh\phi = \frac{Z\rho}{2c_s} \equiv y, \tag{8}$$

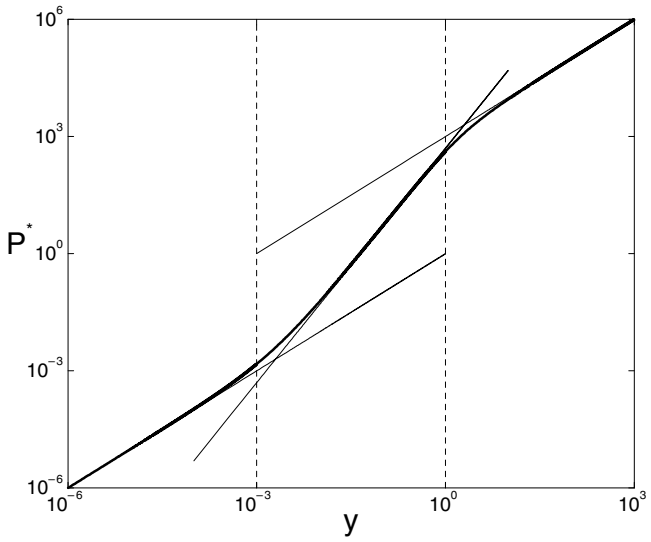

Figure 1. Double logarithmic plot of the dimensionless osmotic pressure P^* of equation (9) (thick curve) as a function of dimensionless colloid density y defined in equation (8), for $Z = 1000$. The three thin curves represent the three regimes identified in equation (10), and show two linear regimes ($y < 1/Z$ and $y > 1$) separated by a quadratic regime $1/Z < y < 1$.

which implies that $\phi = \log(-y+\sqrt{1+y^2})$ is uniquely determined by the dimensionless colloid density y. Insertion of this result into equation (6) yields $c_\pm$ explicitly as a function of y, i.e. as a function of Z, ρ, and c_s. Within the ideal-gas approximation the osmotic equation of state follows as $P/kT = \rho + c_+ + c_- - 2c_s$ [6], the dimensionless form of which is rewritten as

$$P^* = \frac{PZ}{2c_s kT} = y + Z(\cosh\phi - 1)$$
$$= y + Z\left(\sqrt{1+y^2} - 1\right) \tag{9}$$
$$= \begin{cases} y, & y \ll Z^{-1}; \\ Zy^2/2, & Z^{-1} \ll y \ll 1; \\ (Z+1)y, & y \gg 1. \end{cases} \tag{10}$$

Of course these three density regimes are only distinct for highly charged colloids, for which $Z \gg 1$. We illustrate the existence of these three density regimes in figure 1 for $Z = 1000$, where the dimensionless osmotic pressure P^* is plotted (on a log–log scale) as a function of the dimensionless colloid density y. The three regimes are separated by the dashed vertical lines at $y = 1/Z$ and 1, where the crossovers take place. The low-density regime $y < 1/Z$ (or equivalently the high-salt regime), shows a linear equation of state, $P = kT\rho$, i.e. the Donnan equilibrium reduces to the well-known Van't Hoff limit. Also the high-density (or low-salt) regime $y > 1$ exhibits a linear equation of state, $P = (Z+1)kT\rho$. This form suggests that not only the colloids but also the Z counterions per colloid act as independent ideal 'kinetic' units. The intermediate regime, $1/Z < y < 1$, is characterised by a purely quadratic equation of state, $P = kTZ^2\rho^2/4c_s$, i.e. *not* a sum of a linear and a quadratic term as in the lowest-order virial expansion.

3. Sedimentation equilibrium of charged colloids

We can now combine expression (9) for the osmotic pressure of a bulk suspension of charged colloids with the condition of hydrostatic equilibrium given in equation (1). It turns out that analytic results can be found for all three regimes given in equation (10). Fixing c_s and Z, introducing the dimensionless density profile $y(x) = Z\rho(x)/2c_s$, and using the relationship $\mathrm{d}P/\mathrm{d}\rho = kT\,\mathrm{d}P^*/\mathrm{d}y$, we obtain

$$y(x) = \begin{cases} y_0^{(1)} \exp\left(-\dfrac{x}{L}\right), & y < Z^{-1}; \\ y_0^{(2)} - \dfrac{x}{ZL}, & Z^{-1} < y < 1; \\ y_0^{(3)} \exp\left(-\dfrac{x}{(Z+1)L}\right), & y > 1. \end{cases} \tag{11}$$

Here L is defined in equation (2), and $y_0^{(i)}$ represents the integration constant in each of the three regimes, with $i = 1, 2, 3$. Of course two of these can be fixed by imposing continuity at the two crossovers at $x = x_1$ and x_2, defined such that $y(x_1) = 1$ and $y(x_2) = 1/Z$. Straightforward analysis yields that the height of the linear regime is given by $x_2 - x_1 = (Z-1)L$, and that one can write

$$y(x) = \begin{cases} \dfrac{1}{Z} \exp\left(-\dfrac{x - x_2}{L}\right), & x > x_2; \\ 1 - \dfrac{x - x_1}{ZL}, & x_1 < x < x_2; \\ \exp\left(-\dfrac{x - x_1}{(Z+1)L}\right), & x < x_1. \end{cases} \tag{12}$$

This function is plotted in figure 2, for the case $Z = 1000$ and $y(0) = \exp(1)$, i.e. $x_1 = (Z+1)L$ and $x_2 = 2ZL$. The dashed curves indicate $y = 1$ and $1/Z$, where the crossovers take place. Note that the derivative $y'(x) = \mathrm{d}y(x)/\mathrm{d}x$ of the functional form for $y(x)$ of equation (12) is continuous at $x = x_2$, and almost continuous at x_1 for large Z, since $L(y'(x_1^+) - y'(x_1^-)) = \mathcal{O}(1/Z)$. The important observation to make now is that despite the fact that we work on the ideal-gas level (but with the Donnan potential combined with global charge-neutrality built in to account for the Coulombic interactions), we find that the expected barometric distribution (2) only holds in the low-density (high-salt regime) $y < 1/Z$; the density profile is linear in the height x in the regime where $1/Z < y < 1$, and exponential with a decay length equal to $(Z+1)L$ in the regime $y > 1$. In other words, the colloidal density is, in the latter two regimes, much more homogeneous than expected on the basis of the barometric law: the colloids are lifted upwards.

The mechanism that is responsible for this lift effect can readily be identified by combining equations (8) and (12), together with the limits $\sinh\phi \simeq \phi$ for $|\phi| \ll 1$ and $\sinh\phi \simeq -\exp(-\phi)/2$ for $\phi \ll -1$. This yields

$$\phi(x) = \begin{cases} -\dfrac{1}{Z} \exp\left(-\dfrac{x - x_2}{L}\right), & x > x_2; \\ -1 + \dfrac{x - x_1}{ZL}, & x_1 < x < x_2; \\ -\log 2 + \dfrac{x - x_1}{(Z+1)L}, & x < x_1. \end{cases} \tag{13}$$

In words, in the nonbarometric regime $x < x_2$ the local Donnan potential $\psi(x) = kT\phi(x)/e$ is *linear* in x, implying the existence of a homogeneous electric field $E = -\mathrm{d}\psi/\mathrm{d}x$ pointing

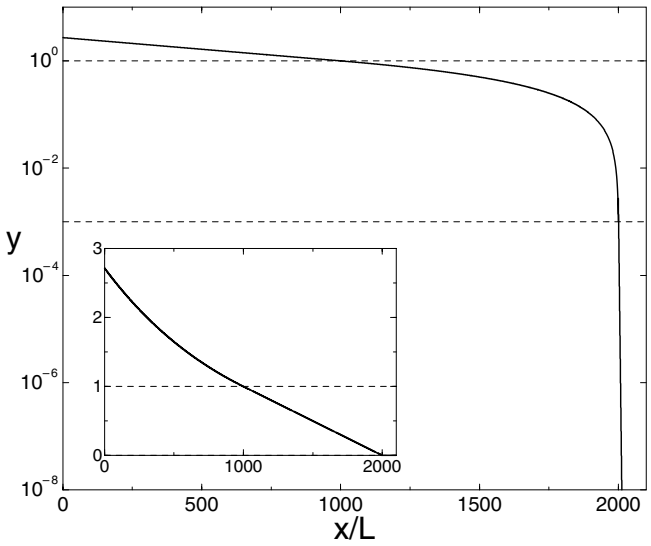

Figure 2. Universal dimensionless sedimentation profile for $Z = 1000$ showing the three regimes (i) an exponential regime with decay length $(Z + 1)L$ for $y > 1$ (at $x < ZL$), (ii) a linear regime with slope $1/ZL$ for $1/Z < y < 1$ (at $ZL < x < 2ZL$), and (iii) an exponential (barometric) regime with decay length L for $y < 1/Z$ (at $x > 2ZL$). The inset shows the same function on a linear scale in order to reveal the linear part more clearly.

downwards, i.e. pushing up the (negative) colloids. In the regime of the linear profile, $x_1 < x < x_2$, this field is given by $E = -mg/Ze$, i.e. the electric force on the colloids $-ZeE = mg$ cancels the gravitational force $-mg$ exactly. In the regime $x < x_1$ the electric force equals $mgZ/(Z + 1)$, and here the balance of electrostatic and gravitational force on a colloid leads to a net downward force $-mg/(Z + 1)$, i.e. as if the colloidal mass is reduced by a factor $Z + 1$. The latter observation was also made in [7–10], on the basis of the Poisson–Boltzmann equation and/or Donnan equilibrium. Note that $\phi(x)$ given in equation (13) is *not* continuous at $x = x_1$. This is unphysical and reflects the asymptotic character of the three regimes; the full (numerically obtainable) solution is of course smooth. The magnitude of the discontinuity of $\phi(x_1)$ is a consequence of our choice to impose a continuous $y(x)$ in equation (12).

4. Charge separation

The existence of a macroscopic electric field in a suspension must be caused by a separation of charges, i.e. by a local violation of charge neutrality (of course charge neutrality must be satisfied globally). The analysis of section 3 is, however, based on the combination of equations (1) and (10), i.e. on local charge neutrality as the bulk equation of state (10) holds for a charge neutral system. In other words, merely combining the bulk equation of state with hydrostatic equilibrium leads to an internal inconsistency. This inconsistency can be repaired if one includes the so-called Maxwell stress to the force balance [11]. One recalls that the mn-component of the Maxwell stress tensor τ is given by $\tau_{mn} = (\epsilon/4\pi)[-E_m E_n - B_m B_n + \frac{1}{2}\delta_{mn}(E^2 + B^2)]$, and that the integral of τ over a closed surface equals the force on the enclosed volume [11]. Here ϵ is the dielectric constant of the suspending medium, E and B are the electric and magnetic field, respectively, and δ_{mn} is the Kroneker delta.

In the sedimentation geometry of present interest only $\tau_{xx} = -(\epsilon/8\pi)E_x^2$ is nonvanishing, and hence the total force Π per unit area (due to interactions in the suspension) can be written as $\Pi = P + \tau_{xx}$, which we rewrite with $E_x = -\psi'(x)$ and the equations (9) and (7) as

$$\beta\Pi(\rho(x), \phi(x)) = \rho(x) + 2c_s(\cosh\phi(x) - 1) - \frac{1}{8\pi\lambda_B}(\phi'(x))^2. \tag{14}$$

Here $\lambda_B = e^2/\epsilon kT$ is the Bjerrum length. The force balance, or hydrostatic equilibrium, in the Earth's gravity field is now given by equation (1) but with P replaced by Π. This yields

$$\frac{\mathrm{d}\beta\,\Pi(\rho(x), \phi(x))}{\mathrm{d}x} = \rho'(x) - Z\rho(x)\phi'(x) = -\frac{\rho(x)}{L}, \tag{15}$$

where the gravitational length L is defined in equation (2), and where we used the Poisson–Boltzmann equation

$$\phi''(x) = \kappa^2 \sinh\phi(x) + 4\pi\lambda_B Z\rho(x), \tag{16}$$

with $\kappa^2 = 8\pi\lambda_B c_s$. A straightforward integration of equation (15) yields the Boltzmann distribution

$$\rho(x) = \rho_0 \exp(-x/L + Z\phi(x)), \tag{17}$$

where ρ_0 is a constant of integration determined by the total amount of colloidal material in the sample. The form (17) for the colloidal density profile is a direct generalisation of the barometric distribution (2) to include electrostatic interactions—it also follows from minimising a mean-field density functional [9]. The main difference between (2) and (17) is that the former is an explicit form for the density profile, whereas the latter is a single equation for the two unknown profiles $\rho(x)$ and $\phi(x)$. The second relation between them is provided by the Poisson–Boltzmann equation (16). The equilibrium profiles $\rho(x)$ and $\phi(x)$ can therefore be solved numerically from the two coupled nonlinear equations (16) and (17), subject to appropriate boundary conditions. The symbols in figure 3 represent, for several reservoir salt concentrations c_s, the resulting dimensionless density profiles $\eta(x) = (\pi/6)\rho(x)\sigma^3$, i.e. the packing fraction, of a suspension of charged spheres with $Z = 200$, diameter $\sigma = 150$ nm, $\lambda_B = 2.3$ nm (ethanol at room temperature), and gravitational length $L = 2$ mm. The suspension is confined (by the solvent volume) to $0 < x < H$ with $H = 20$ cm, with electrostatic boundary conditions such that $\psi'(0) = \psi'(H) = 0$, and with the normalisation given by the total packing fraction $(1/H)\int_0^H \mathrm{d}x\,\eta(x) = 0.0005$ in all cases. The curves in figure 3 represent, for the same parameters, the packing fraction profiles that result from a numerical integration of equation (1) with $P(\rho)$ the Donnan bulk pressure of equation (9), i.e. the inconsistent approximation that $\phi'(x) \equiv 0$ is made (but here the full expression for P is used instead of the three asymptotic regimes given in equation (10)). The agreement between the Poisson–Boltzmann (symbols) and the Donnan-based profiles (lines) is remarkably good, but *not* exact of course. Note that the former follow from a second-order system of differential equations, and the latter from a first-order differential equation, i.e. the latter requires substantially less numerical effort to obtain. The (small) difference between the two density profiles can be seen more clearly in figure 4, to be discussed later.

In figure 3 the parameters Z, σ, λ_B, L, as well as the average packing fraction, correspond to a good approximation to the supernatant phases observed in [10]. At the highest salt concentration, $c_s = 10^{-3}$ M, the profile is indistinguishable from the barometric distribution (2), indicating that local charge neutrality applies. At lower salt concentrations, $c_s \leqslant 10^{-5}$ M, (i.e. at larger y) a linear part appears in the profiles, of which the slope decreases with c_s as given by equation (12). The linear part does *not* span the whole sample for $c_s = 10^{-5}$ M and 10^{-6} M, where a crossover takes place to the barometric regime at that

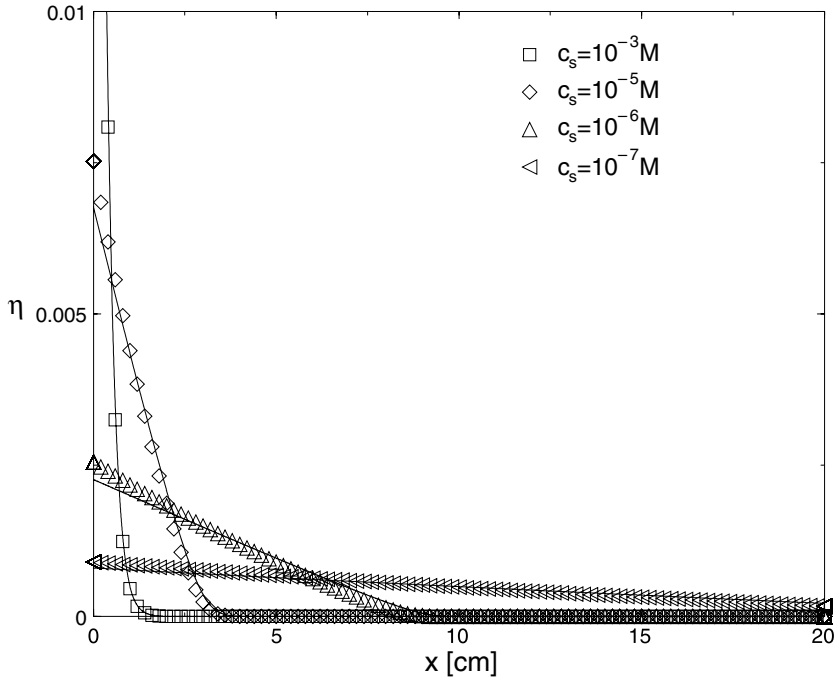

Figure 3. Predicted packing fraction profiles in a sample of height $H = 20$ cm with an average packing fraction 0.0005 for several salt concentrations c_s. The symbols represent the Poisson–Boltzmann-based profiles, and the lines the Donnan-based ones. The colloidal charge is $Z = 200$, the Bjerrum length $\lambda_B = 2.3$ nm is that for ethanol at room temperature, the gravitational length is $L = 2$ mm, and the colloidal diameter is $\sigma = 150$ nm. These parameters are close to the experiments of [10], where probably $c_s < 10^{-7}$ M. The curves reveal that the density profile becomes more homogeneous as the salt concentration c_s is lowered, and that the inconsistent Donnan-based profiles are a good approximation of the full (consistent) Poisson–Boltzmann results.

height x where $y(x) = 1/Z$. For $c_s = 10^{-7}$ M, which we consider an upper bound for the experimental salt concentration in [10], the linear regime spans the whole sample. It is tempting to explain the observed strong scattering, which signifies the presence of a finite concentration of colloids, in the supernatants of [10] by the present theory. This remains, however, to be confirmed, e.g. by a direct measurement of an electric field in these systems [12].

Whether or not the linear regime spans the whole sample has a profound effect on the total charge-density $-Z\rho(x) - 2c_s \sinh \phi(x)$, which is represented (in arbitrary units) by the thick curves in figure 4 for (a) $c_s = 10^{-6}$ M and (b) $c_s = 10^{-7}$ M. Figure 4 also shows the corresponding colloid density profiles (symbols for Poisson–Boltzmann results and thin line for Donnan-based results). Figure 4 reveals that the net local charge is either strongly localized in the very edges of the system $x \simeq 0, H$ (in layers with a thickness of the order of the Debye-length κ^{-1}, see the inset in (b)), or rather broadly distributed below the crossover $y = 1/Z$ (inset of (a)), where the linear and the barometric regime meet. In both of the cases (a) and (b) there is a condenser effect that pushes the colloidal particles upward. This effect was also described in [7–9].

In the case of the strongly localized charge distribution at the bottom of the container (and at the top in the case that the linear regime spans the whole sample) it is of interest to consider the magnitude of the corresponding surface charge density. At the end of section 3 we found

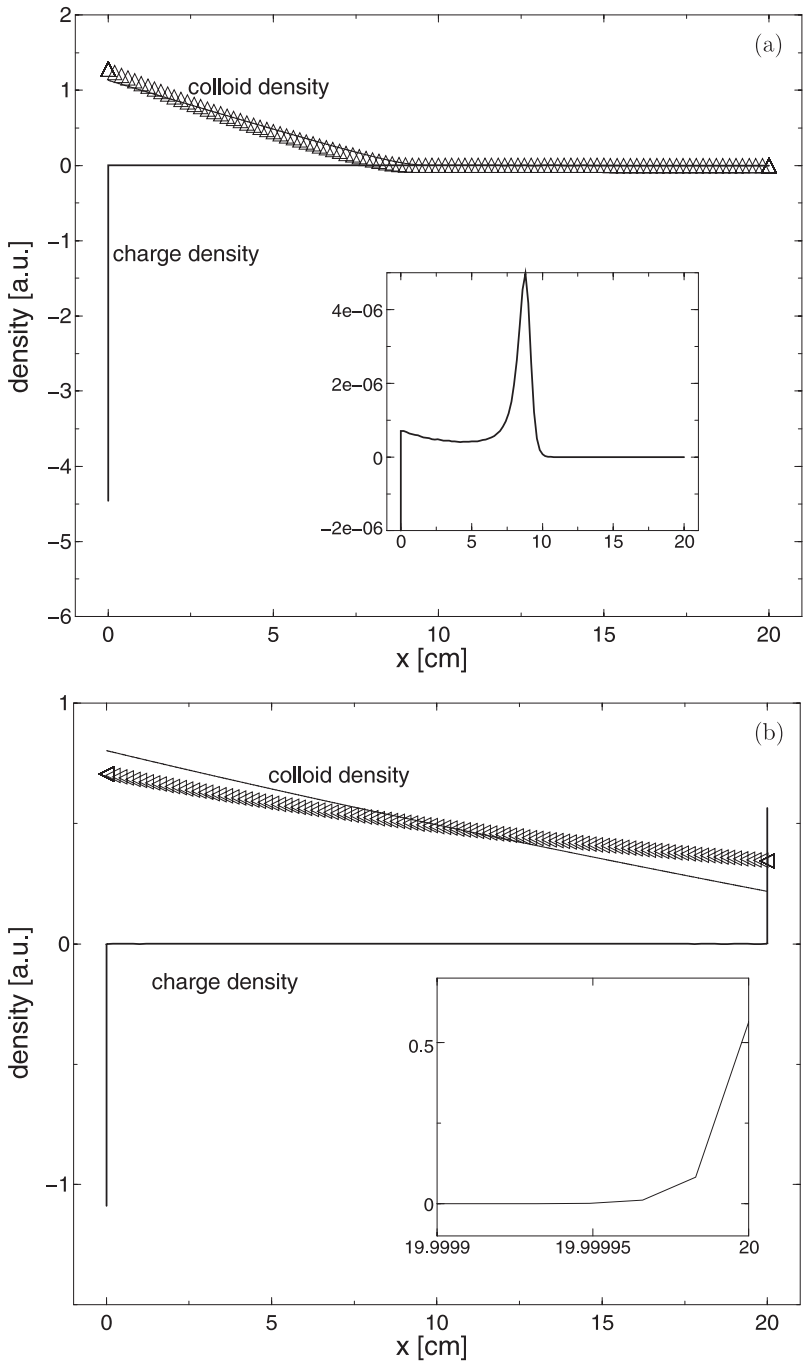

Figure 4. Colloidal density (symbols and thin curves as in figure 3) and total charge-density (thick curves), in arbitrary units, for the same parameters as in figure 3, with (a) $c_s = 10^{-6}$ M and (b) $c_s = 10^{-7}$ M. In (a) the net positive charge is broadly distributed in $0 < x$ (cm) < 10, whereas in (b) it is strongly confined to a thin layer in the top (with a thickness of the order of the Debye length κ^{-1}). The net negative charge resides at the bottom in both (a) and (b). This negative charge pushes up the (negative) colloids to higher altitudes than expected on the basis of the barometric distribution.

that the electric field that is generated selfconsistently is of magnitude $E = mg/(Ze)$ for large Z. It follows from elementary electrostatics that the corresponding area a per net charge is $a/e = 4\pi/(\epsilon E)$, from which the area a follows as

$$a = 4\pi Z\lambda_B L. \tag{18}$$

Inserting typical numbers, e.g. $Z = 10^3$, $\lambda_B = 1$ nm and $L = 1 - 10^3$ μm, yields an area as large as $a \simeq 10 - 10^4$ μm^2. Such a large area, or such a low surface charge density, is a direct manifestation of the relatively strong Coulomb force compared to gravity: it does not take much charge to counteract the gravitational force.

5. Discussion

An important question is now whether, or to what extent, the regimes $y > 1$ and $Z^{-1} < y < 1$ are experimentally accessible, and to what extent a Donnan-like ideal-gas type analysis is appropriate. In order to analyse these questions we rewrite y from equation (8) as

$$y = 24\eta \frac{Z\lambda_B}{\sigma} \frac{1}{(\kappa\sigma)^2}. \tag{19}$$

Here we used the previously introduced colloidal packing fraction η, the Bjerrum length λ_B, the colloidal diameter σ, and the reservoir screening length κ^{-1}. Typical colloidal parameters are $\sigma = 0.1$–1 μm, $\lambda_B = 1$–10 nm, and $Z = 100$–1000, and hence $Z\lambda_B/\sigma \simeq \mathcal{O}(1)$. The regime of physical (and detectable) packing fractions is, typically, $\eta \simeq 10^{-5}$–10^{-1}, and $\kappa\sigma = 10^{-1}$–10^4 for salt concentrations ranging from the extremely low $c_s \simeq 10^{-9}$ M (in organic solvents) to the saturation value $c_s \simeq 10$ M (in water). These numbers imply that $y > 1$ is possible in the low-salt regime $\kappa\sigma \leqslant 1$, e.g. for $\kappa\sigma = 1$ when $\eta > 0.05$, or for $\kappa\sigma = 0.1$ when $\eta > 0.0005$. Moreover, and perhaps more interestingly, the regime $y > 1/Z$ is much more easily accessible, e.g. for $Z = 1000$ even at $\kappa\sigma = 10$ when $\eta > 0.005$.

The question whether or not the colloid–colloid interactions can be ignored, as we do here, can be estimated by a calculation of the osmotic second virial coefficient $B_2 = (1/2)\int \mathrm{d}\mathbf{r}\,(1 - \exp(-v(r)/kT))$, where $v(r)$ is the effective colloidal pair interaction. If one assumes that this potential is given by the DLVO-like screened-Coulomb form [13]

$$v(r) = \begin{cases} \infty, & r < \sigma; \\ \dfrac{Z^2e^2}{\epsilon} \dfrac{\exp(\kappa\sigma)}{(1+\kappa\sigma/2)^2} \dfrac{\exp(-\kappa r)}{r}, & r > \sigma, \end{cases} \tag{20}$$

one straightforwardly calculates B_2 numerically. A rough estimate of the crossover density from the ideal-gas to the interacting regime is then given by $B_2\rho = 1$.

In figure 5 we present a log–log plot of the curve $B_2\rho = 1$ in the (η, c_s) plane, together the lines $y = 1/Z$ and 1. Given the large number of decades displayed, one can view $B_2\rho = 1$ as a rough estimate of the freezing line; in the high-salt (hard-sphere) limit this yields $\eta = 0.25$, a mere factor two from the well-known actual hard-sphere freezing transition. The parameters in figure 5(a) are $\lambda_B = 2.3$ nm, $\sigma = 150$ nm, and $Z = 100$, all closely related to the experiments of [10]. The parameters in figure 5(b) are $\lambda_B = 7.2$ nm, $\sigma = 2.16$ μm, and $Z = 2300$, which correspond to another experimental system that is presently investigated [14]. In both cases, and actually in all other cases that we studied, the regime $y > 1$ is completely masked by $B_2\rho > 1$. This implies that a realistic study of this regime must take into account the effective colloidal interactions. By contrast, in both (a) and (b) as well as in all other cases that we studied we find that the intermediate density regime $1/Z < y < 1$, i.e. the regime where we predict macroscopic electric fields in sedimentation equilibrium, has a substantial part in the ideal-gas-like regime $B_2\rho < 1$. This observation indicates that the presently used ideal-gas approach is sufficiently accurate to realistically describe the selfconsistent macroscopic

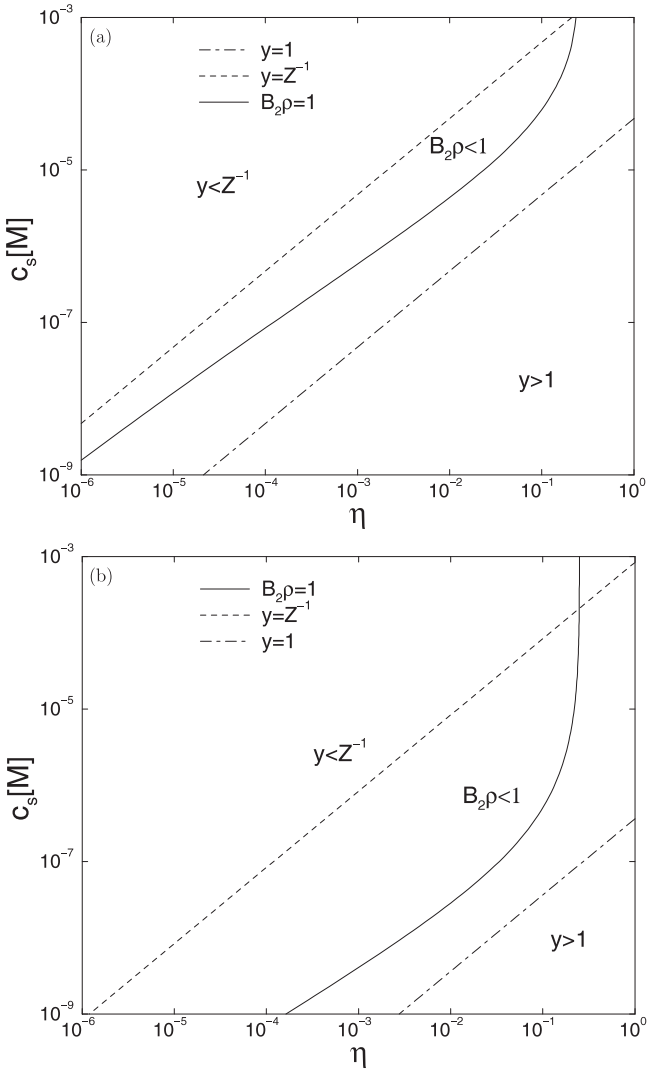

Figure 5. Separation of (η, c_s) plane into the low-density regime $y < Z^{-1}$, the low-salt regime $y > 1$, and the weak-interaction regime $B_2\rho < 1$, where η is the colloidal packing fraction, c_s the reservoir salt concentration, Z the colloidal charge number, and y the dimensionless colloid density defined in equation (8). Parameters are (a) $Z = 100$, $\lambda_B = 2.3$ nm, and $\sigma = 150$ nm similar to the experiments in [10], and (b) $Z = 2300$, $\lambda_B = 7.2$ nm, and $\sigma = 2160$ nm as in experiments of [14]. Note that the low-salt regime $y > 1$ is in the strong-interaction regime in both (a) and (b).

electric field that pushes up the colloids to relatively large heights compared to the barometric distribution. In other words, we conclude that the macroscopic electric field predicted here and in [7–9] could well be a real phenomenon, and could be detectable experimentally [12].

We wish to end with a qualitative, rather handwaving thermodynamic explanation of the electric field in sedimentation equilibrium. In a one-component fluid sedimentation equilibrium is the result of the competition between gravity (favouring all particles at the bottom) and entropy (favouring a homogeneous distribution), and the balance yields, for a dilute system, the exponential barometric distribution (2). In a mixture of (massive) charged colloids

and (massless) cations and anions the situation is more complicated, and actually frustrated: gravity favours the colloids at the bottom, but *not* the cations and anions, whereas electrostatics favours local charge neutrality, while entropy favours a homogeneous distribution. At high salt concentrations the entropic cost of satisfying local charge neutrality, even at the bottom where most of the colloids prefer to be, is limited, since only a small fraction of the ions is needed to compensate the colloidal charge, i.e. the ion fractionation is small and hence entropically 'cheap'. By contrast, at low ion concentrations a large fraction of the ions, or almost all of them, would be required to attain local charge neutrality at the bottom (where the colloids would be), and the corresponding fractionation of the ions into a dense layer at the bottom and a dilute one on top would be entropically 'expensive'. In this low-salt limit the free energy balance is therefore dominated by the ion entropy, and the free energy is optimised by sacrificing the local charge neutrality to set up an electric field pushing up the colloids, and hence allowing for a colloid and ion density distribution that is much more homogeneous than predicted by the barometric law.

This entropic lift effect is a genuine many-body effect, that seems to be difficult to catch within an effective one-component description of the suspension. Such a description is based on an effective Hamiltonian H for N charged colloids at positions $\mathbf{R}_i$ (with $i = 1, \ldots, N$) in osmotic contact with a salt reservoir. In the presence of an external potential (such as the gravitational potential of interest here) H can be shown to take the general form [15]

$$H = \sum_{i=1}^{N} v_1(\mathbf{R}_i) + \sum_{i<j}^{N} v_2(\mathbf{R}_i, \mathbf{R}_j) + \sum_{i<j<k}^{N} v_3(\mathbf{R}_i, \mathbf{R}_j, \mathbf{R}_k) + \cdots, \tag{21}$$

where v_n is the n-body potential, defined in the n-colloid system and hence independent of the colloid density [15]. Since $y = Z(n/V)/(2c_s) \ll 1/Z$ for any microscopic n and macroscopic volume V, the potentials are all defined in the low-density (Van't Hoff) regime as long as $n \ll 2c_sV/Z^2$. In other words, *no* entropic lift effect in the Earth's gravity field will be predicted for any reasonable truncation of the expansion of equation (21). One might speculate that an effective one-component Hamiltonian of the form (21) can neither deal properly with other inhomogeneities in suspensions of charged colloids, e.g. interfaces of coexisting phases or wetting films, since the possibility of local charge separation is an intrinsically multi-component feature. Rather one should then consider such inhomogeneities directly at the level of density profiles and the free energy instead of the effective Hamiltonian. We plan to investigate this in more detail in future work.

Acknowledgments

It is a pleasure to thank Albert Philipse, Gijsje Koenderink, Marjolein Dijkstra, Antti-Pekka Hynninen, Mirjam Leunissen, Paddy Royall, Alfons van Blaaderen, and Henk Lekkerkerker for stimulating discussions. Henk Lekkerkerker is also thanked for suggesting the derivation of equation (17) through the inclusion of the Maxwell stress. This work is part of the Research program of the 'Stichting voor Fundamenteel Onderzoek der Materie (FOM)', which is financially supported by the 'Nederlandse Organisatie voor Wetenschappelijk Onderzoek (NWO)'.

References

[1] Yang A J M, Fleming P D and Gibbs J H 1977 *J. Chem. Phys.* **67** 74
[2] Piazza R, Bellini T and Degiorgio V 1993 *Phys. Rev. Lett.* **71** 4267
[3] Vrij A 1980 *J. Chem. Phys.* **72** 3735

[4] Biben T, Hansen J-P and Barrat J-L 1993 *J. Chem. Phys.* **98** 7330
[5] Löwen H 1998 *J. Phys.: Condens. Matter* **10** L479
[6] Mysels K J 1967 *Introduction to Colloid Chemistry* (New York: Wiley)
[7] Biben T and Hansen J-P 1994 *J. Phys.: Condens. Matter* **6** A 345
[8] Simonin J-P 1995 *J. Phys. Chem.* **99** 1577
[9] Téllez G and Biben T 2000 *Eur. Phys. J.* E **2** 137
[10] Philipse A P and Koenderink G H 2003 *Adv. Colloid Interface Sci.* **100–102** 613
[11] Ohanian H C 1988 *Classical Electrodynamics* (Boston, MA: Allyn and Bacon)
[12] Philipse A P and Erné B 2003 private communication
[13] Derjaguin B and Landau L 1941 *Acta Physicochim. URSS* **14** 633
Verwey E J W and Overbeek J Th G 1948 *Theory of the Stability of Lyotropic Colloids* (Amsterdam: Elsevier)
[14] Leunissen M and van Blaaderen A 2003 private communication
[15] Russ C, von Grünberg H, Dijkstra M and van Roij R 2002 *Phys. Rev.* E **66** 011402